Neuronal numbers in the frontal cortex of a novel transgenic mouse model of Alzheimer's Disease

Marijke LEMMENS

promotor :
dr. C. SCHMITZ

Eindverhandeling voorgedragen tot het bekomen van de graad
Master in de biomedische wetenschappen afstudeerrichting
klinische en moleculaire wetenschappen

Universiteit Maastricht

universiteit hasselt

"Death is not the greatest loss in life. The greatest loss is what dies inside us while we live."

(Norman Cousins)

Table of contents

List of abbreviations

AD – Alzheimer's Disease

Aβ – Amyloid β

APLP – Amyloid Precursor-Like Proteins

ApoE – Apolipoprotein E

APP – Amyloid Precursor Protein

C38 – 83-residue COOH-terminal fragment

C99 – 99-residue COOH-terminal fragment

CA – Cornu Ammonis

FAD – Familial Alzheimer's Disease

Ho – Homozygous

He – Hemizygous

KI – Knock-in

PDGF-β - Platelet-Derived Growth Factor-β

PrP – Prion Protein Promoter

PS – Presenilin

SAD – Sporadic Alzheimer's Disease

SL – Swedish and London mutation

SEM – Standard Error of the Mean

Thy – Thymidine

Preface

The study described in this thesis was performed during my Master internship in the Department of Psychiatry and Neuropsychology, Division of Cellular Neuroscience in Maastricht University (Maastricht, the Netherlands). It was my goal to do my internship on a subject that really matters to me. For that reason, I decided to dive into the field of Alzheimer's Disease.
In my opinion, the brain is the most important organ in the human body. Of course, the heart and lungs are vital organs as well and one cannot live without them; nevertheless, the brain is the most essential of all to me. For example, if one has a heart disease, medication or hospitalization can provide the solution in most cases. Anyhow, one can talk with his relatives and be aware of everything that happens in the surroundings. However, when suffering from Alzheimer's Disease, dementia and both cognitive and motor impairments are inevitable. One loses his identity and is in great risk of becoming a burden on relatives and loved ones. For me, this is the worst thing than can happen to a person and for this reason, I was very interested in working on this topic.
Choosing the Department of Psychiatry and Neuropsychology, runned by Prof. Dr. Harry Steinbusch, was the logical thing to do for me, based on my Major internship I did here in the last year of my Bachelor studies. I enjoy the way of working in this department. There is a good interaction between the various groups, scientifically as well as socially. I enjoy exchanging my knowledge with others in order to broaden my horizon.
Lastly, I chose to work for Dr. Christoph Schmitz because in my opinion, this group will offer me the most opportunities. I want to be successful in my further scientific career and this group will hopefully provide the basis for that.

This study and the resulting thesis was established with the help of several co-workers.
I would like to thank Prof. Dr. Harry Steinbusch for allowing me to work in the Department of Psychiatry and Neuropsychology and for his excellent guidance. Furthermore, I want to thank my promotor Dr. Christoph Schmitz for sharing his extensive knowledge with me and also for giving me the opportunity to explore already a part of the scientific world.
Also great thanks to my friends and fellow-students, Eveline Strackx, Dorien Merken and Silvie Timmers for their advise and their friendship during these past six months. In addition, the PhD-students in the group of Dr. Christoph Schmitz, Imke van Kooten, Pawel Kreczmanski and Ivona Brasnjevic, who always answered all of my questions with the same enthusiasm.
For the technical assistance, I want to express my gratitude to the technicians in our lab, Marjanne Markerink and particularly Hellen Steinbusch. Performing this study without them would have been a lot more difficult.
And last but not least, I want to thank my parents and the rest of the family for their support and for giving me the opportunity to do these studies.

Abstract

Alzheimer's Disease (AD) is neurodegenerative disorder, characterized by extracellular plaques, intracellular tangles and synaptic and neuronal loss in selective brain regions.

In the present study, we investigated the frontal cortex of APP/PS1 KI mice, a novel transgenic mouse model of AD. The APP/PS1 KI mice overexpress human amyloid precursor protein (APP) with the Swedish and London mutations and carry M233T/L235P knocked-in mutations in presenilin 1 (PS1). This model has shown in a previous study a substantial neuron loss in the CA1/2 pyramidal cell layer that correlated more with intraneuronal Aβ and Thioflavine S-positive aggregates than with extracellular Aβ deposits.

In this study, the volume and the neuron numbers of the frontal cortex in APP/PS1 KI mice were assessed using design-based stereology. In the frontal cortex of APP/PS1 KI mice, a neuron loss of 28% was detected in layers V-VI at 10 months of age. In addition, the plaque load in these mice in layers V-VI was 11%. Thus, the amount of plaques present in the frontal cortex of these animals does not fully account for the extent of observed neuron loss. As a possible key mediator in this mechanism, the intraneuronal accumulation of Aβ is proposed. Using an Aβ and Thioflavine S double staining, intraneuronal Aβ and Thioflavine S-positive deposits were observed in layers V-VI pyramidal neurons.

The APP/PS1 KI mice are concluded to be a excellent model for investigating the pathology in AD, with a substantial neuron loss in different brain regions and modelling the critical role of intraneuronal Aβ in neuron loss. Therefore, this model is an excellent tool for further research about the pathogenesis of AD and possibly testing potential therapeutics.

1 Introduction

In this study, the frontal cortex of a novel mouse model of Alzheimer's Disease (AD) was investigated. It is already known from this particular mouse model that there are aberrations present in the hippocampus (1). Therefore, we were interested to see if other brain regions known to be affected in AD had the same symptoms. We decided to address volume and neuron numbers of the frontal cortex in this mouse model to assess the extent of AD-like pathology present in this mouse model.

In the first part of the introduction, a general overview is given about AD and its pathology. Subsequently, the phenomenon of selective neurovulnerability in AD is explained. Next, several transgenic mouse models that have been developed over the years are summarized. The last section of the introduction is an outline of the current study.

1.1 Alzheimer's Disease

Alzheimer's Disease (AD) is a devastating disease, which was mentioned for the first time in a paper by Alois Alzheimer, in 1907 (2). AD is characterized by two chief hallmarks: extracellular amyloid-β (Aβ) deposits, the so-called plaques, and the formation of intracellular neurofibrillary tangles (3,4). The plaques consist mainly of insoluble Aβ aggregates, whereas hyperphoshorylated Tau proteins form the tangles (5). Further neuropathologies are neuronal and synaptic dysfunction and loss of neurons and synapses. The behavioural symptoms of AD are memory loss and general cognitive decline. As the disease progresses, these symptoms can aggravate to motor complications and the disappearance of most personal traits. In the end-stage, AD renders the patients totally dependent on their caregivers (6, 7). According to epidemiological data, the duration of AD can vary between 2 and 20 years (8), with a reported median survival time of 3-4 years (9).

Based on the age of onset, AD can be categorised in two forms:

1. The familial form of AD (FAD) has an early age of onset (< 65 years) and the patients harbor autosomal dominant mutations in specific genes. However, FAD constitutes only 3-5% of all AD cases (10). Mutations playing a role in AD are identified in three genes: genes for amyloid precursor protein (APP) (11), presenilin 1 (PS1) and presenilin 2 (PS2) (12, 13).
2. Sporadic AD (SAD) is the late onset (> 65 years) form of AD. In these patients' DNA, no single mutations have been identified yet (10).

Importantly, ApoE4 gene polymorphism is correlated with both familial and sporadic forms of AD. Patients with either one or two of these alleles have a two- to fivefold increased risk of AD, respectively (14) .

Currently, the number of people in the world that suffer from dementia, irrespective of the cause, is 24.3 million (15). About 75% of this number is due to AD, with women having a higher prevalence than men (8,16). When taking age into account as the greatest risk factor for AD and considering the increased life span of humans nowadays, it is expected that the number of AD cases will double over the next 20 years (15).

Despite growing interest and research, AD still remains a disease which conceals a lot of unanswered questions. The precise etiopathogenesis is currently still largely unknown. Several hypotheses have arisen over the past years about the precise pathologic mechanism leading to AD and its symptoms. A variety of findings about mutations in the FAD genes enhancing the formation of amyloid-β (Aβ) as well as *in vitro* evidence for the neurotoxicity of Aβ (17, 18) are the foundations of the so-called Aβ cascade hypothesis. This hypothesis holds that altered amyloid processing and aggregation is the main mechanism in the pathogenesis of AD and the resulting changes cause all other described pathologies in the AD brain, such as tangles and both synapse and neuron loss (18, 19).

In the Aβ cascade hypothesis, one of the most important molecules is the amyloid precursor protein (APP) (Fig.2). This protein is a member of the family of ubiquitously expressed Amyloid Precursor-Like Proteins (APLP), important for neurodevelopment and neuronal migration (20). APP is a single transmembrane polypeptide with an intracellular C-terminal site and a N-terminal site in the extracellular space or the lumen of secretory vesicles.

APP can undergo different proteolytic cleavages (21) (Fig.1):

a. The non-fibrillogenic cleavage by α-secretase releases a large soluble ectodomain fragment (α-APP) in the extracellular environment. In the membrane, a 83-residue COOH-terminal fragment (C83) is retained (22). Consequently, the C83 fragment is cleaved by γ-secretase, a multiprotein complex which comprises PS1 and PS2 (23). The resulting proteins are P6 and P3 in the membrane and the extracellular space, respectively.
b. The alternative, fibrillogenic, cleavage differs from the first in that respect that the APP molecule is cleaved by β-secretase. This results in a 99-residue COOH-terminal fragment (C99) in the membrane (24). Following the cleavage by β-secretase, γ-secretase cleaves the C99 fragment, resulting in an Aβ peptide (either Aβ40 or Aβ42) and a small peptide fragment called P6. Aβ peptide is first located intracellular and moves subsequently to the extracellular space.

Both α-secretase and β-secretase cleavage occur in the normal brain, but in AD, the latter one is more prominent (19). As mentioned above, the Aβ peptides, resulting from subsequent β-secretase and γ-secretase cleavage, are according to the Aβ cascade hypothesis the key molecules in the pathogenesis of AD. Furthermore, Aβ42 is considered to be more pathogenic than Aβ40 (25).

Aβ deposits can have different morphologies, reflecting different amounts of fibrillar, β-pleated sheet confirmation. Diffuse deposits have little β-pleated sheets, while neuritic plaques are compact, fibrillar deposits displaying a dense core. The latter ones can be stained with

Thioflavine S or Congo Red. Although neuritic plaques constitute only a small number of the plaques, they are far more neurotoxic than the diffuse plaques. Further evidence suggests that only the fibrillar core of the Aβ deposit is toxic (26).

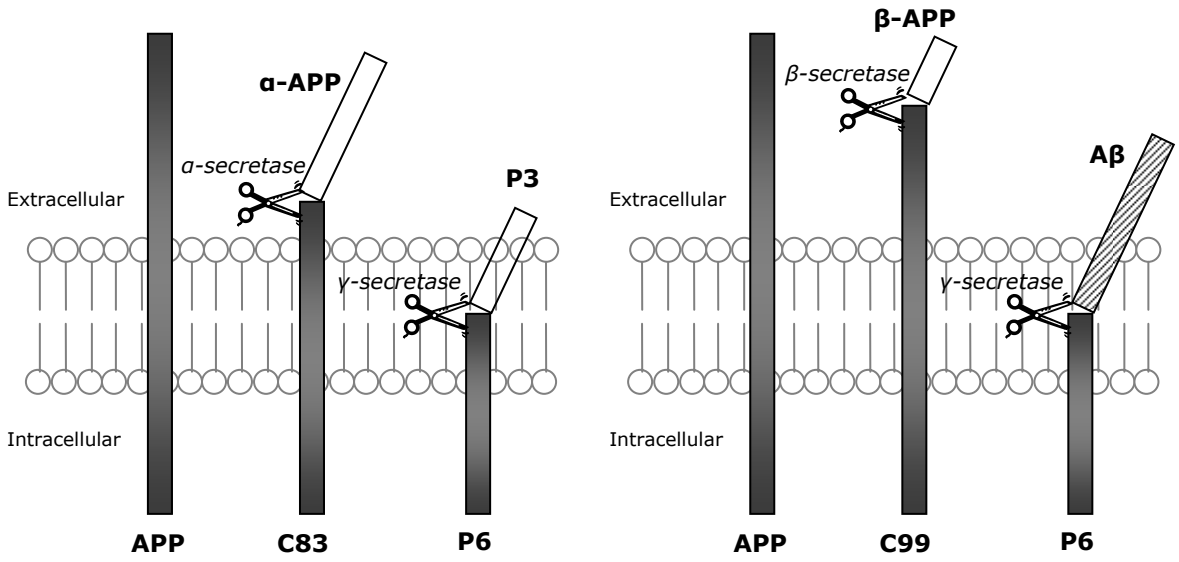

Figure 1. Amyloid precursor protein (APP) and the two main ways of its processing

A. Cleavage of APP by α-secretase (carried out by ADAM10) enabling the secretion of the large, soluble ectodomain of APP (α-APP) and retention of the 83-residue COOH-terminal fragment in the membrane. C83 can also undergo cleavage by γ-secretase (carried out by multiprotein complex) to release the P3 peptide.

B. Proteolytic cleavage of APP by a protease called β-secretase (carried out by BACE-1) resulting in the secretion of the β-APP molecule and the retention of a 99-residue COOH-terminal fragment. The C99 fragment can undergo further cleavage by γ-secretase into Aβ peptide and the P6 fragment.

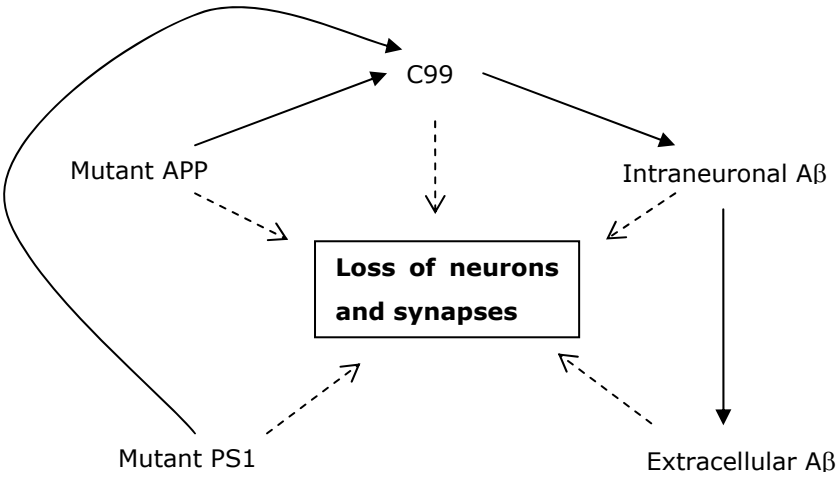

Figure 2. Scheme representing the candidate sources of the neuron and synapse loss in AD, according to the Aβ cascade hypothesis.

The possible players in the Aβ cascade hypothesis are mutated APP or PS1, the accumulation of intra- and extracellular Aβ and the C99 fragment of APP. Mutant APP means that there is an increased level of C99 and increased concentrations of Aβ in neurons and later in the extracellular space. Because PS1 is part of the γ-secretase complex, mutated PS1 enhances this cleavage resulting in elevated levels of Aβ. Dashed arrows mean that the associations are undetermined yet.

1.2 Selective neurovulnerability in the AD brain

AD selectively affects neurons in certain brain regions and neural systems, among which are nerve cells in the frontal cortex and the hippocampus (27),(28). The selective vulnerability of corticocortical and hippocampal circuits was underlined by Morrison and Hof (29).

When reading the literature about neuropathology in mouse models of AD, it is obvious that researchers are particularly interested in the hippocampus. After all, this is a very important area for learning and memory processes, of which alterations are the first symptoms in AD (30). However, the frontal cortex is also known to be important for these functions (31). Indeed, several scientists have reported abnormalities in the frontal cortex in AD, particularly in the large pyramidal neurons of neocortex that extend long corticocortical projections (32-34) and several populations of cortical interneurons (35). These cortical pyramidal neurons seem to be particularly vulnerable, and their death disrupts connections between the association cortices (36). By way of illustration of pyramidal vulnerability, up to 90% of large pyramidal neurons in human prefrontal cortex are lost by the end stages of AD (37).

1.3 Mouse models of AD: single and double transgenic

Transgenic mouse models of AD are designed to emulate the symptoms and pathology of AD (38,39). The goal of this approach is accomplishing a better understanding of the neuropathology of AD and the cognitive changes that go along with it. Furthermore, transgenic mice can be used for testing possible therapies. In the past 15 years, numerous transgenic mouse models of AD have been produced, mostly by altering the FAD-associated genes. Although most of these mouse models have proven to be very useful, none of the developed mouse models exhibit all the symptoms present in the human AD brain yet.

1.3.1 Single transgenic mice

For the creation of transgenic mice that express AD-like pathology, researchers have tried many concepts such as knock-outs, wild-type APP expression or FAD-based APP and PS-mutations. Although many mouse strains have been developed, only a few expressed actual neuropathological marks.

Gene-targeting

Various gene-targeted knock-out mice have been developed in the past. The APP knock-out mouse was generated by Zheng and colleagues in 1995 (40). However, these mice lacked an AD-related phenotype, possibly as a consequence of other proteins of the APLP family taking over the role of APP (21). Next, in 1997, different groups tried to create PS1 knock-out mice (41, 42). Unfortunately, these animals did not survive due to serious congenital physical defects caused by a disturbed development of the axial skeleton. Therefore, in 1997, Shen et al. concluded that PS1 is required for the normal neurogenesis and neuronal survival (41).

Wild-type human APP

Another group of transgenic mouse models of AD was based on the overexpression of wild-type human APP. Although most of these attempts were not successful, some frail results were obtained with the NSEAPP mice (43). In the brain of the NSEAPP mouse, an age-related increase of extracellular diffuse deposits of human Aβ was detected. Later on, a cognitive decline increasing with age was reported in NSEAPP mice (44) but neither astrocytic reaction nor neurodegeneration was ever observed (45).

Mutant human APP

Next, transgenic mice were produced overexpressing mutant human APP. Mutations mostly applied are the so-called double Swedish APP K670N/M671L and London APP V717I mutations. The Swedish mutation is located at the β-secretase cleavage site and renders APP to be a better substrate for β-secretase, resulting in the increased production of Aβ. In contrast, the London mutation occurs at the γ-secretase cleavage site and causes an enhanced production of the Aβ42 peptide. Games and colleagues (46) reported in 1995 a convincing mouse model of AD, the PDAPP mouse. PDAPP mice overexpress human APP with a V717F mutation controlled by a

platelet-derived growth factor β (PDGF-β) promoter. These mice express very high levels of APP protein and develop an AD-like neuropathology including, among others, extracellular diffuse and neuritic plaques and loss of synapse density (46, 47). Furthermore, the amyloid burden as well as memory impairments both increase with aging (48). The amyloid pathology in PDAPP mice resembles that observed in AD. However, these neurodegenerative alterations are not accompanied by global neuronal loss in the entorhinal cortex, CA1, or cingulate cortex through 18 months of age (49).

In 1996, Hsiao et al. (50) published another APP overexpressing mouse model of AD, the Tg2576 line. These mice are transgenic for human APP with the double Swedish mutation under the control of the hamster prion protein promoter *(*PrP). Heterozygous Tg2576 mice produce APP at high levels and develop diffuse and neuritic plaques in the hippocampus, cortex, subiculum, and cerebellum at around 9-11 months of age, similar to those seen in AD and PDAPP mice. Tg2576 mice show subtle age-related memory deficits starting at around 8 months of age (50). However, Tg2576 mice lack global loss of synapses or neurons in CA1 (51).

A third mouse model is the APP23 mouse strain, overexpressing human APP751 carrying the Swedish double mutation under control of the mouse thymidine-1 (Thy-1) promoter. APP23 mice develop both amyloid plaques and cerebral amyloid angiopathy starting at around 6 months of age (52). Similarly to the previously described models, APP23 mice develop memory deficits as assessed by behavioural tests (53). Unlike the PDAPP and Tg2576 lines, a mild neuron loss of 14% was reported in the CA1 of APP23 mice, although no loss was detected in the cortex (54).

Mutant PS

All these models concerning the APP gene can recapitulate much of the amyloid pathology seen in AD. However, APP mutations cause only a tiny percentage of the already small number of FAD cases, as mentioned above. Mutations in presenilins 1 and 2 are also known to cause familial AD (13). They most probably alter the processing of APP with increased production of Aβ as a result as well as an accelerated deposition of amyloid. For this reason, FAD-associated presenilin mutations have also been used to generate animal models. As in the case of APP-transgenic mice, several models have been tested and only a few were successful. Overexpression of either M146L or M146V FAD-associated mutations under the control of PDGF-β promoter cause a selective increase in Aβ42 production but no pathological changes. Furthermore, overexpression of wild-type PS1 does not change Aβ42 levels (55) and PS2 overexpressing mice similarly fail to develop any amyloid pathology (56).

1.3.1 Double transgenic mice

In addition to single transgenic mice, either with alterations in the APP or PS1 gene, double transgenic mice have been developed with a combination of mutations in both FAD genes. As mentioned above, PS1 expression alone is not sufficient to induce amyloid pathology. In research concerning double transgenic mice, PS1 has shown to accelerate plaque deposition when coexpressed with APP. These findings support the role for PS1 as a modifying gene. FAD-associated mutations of presenilins only cause an increased probability of producing the highly fibrillogenic Aβ42 instead of the less harmful Aβ40.

Most of the double transgenic mouse models resulted in an increased Aβ42:Aβ40 ratio and an accelerated amyloid deposition (57-59) but stereological investigation of the hippocampus and frontal cortex of these mice indicate that there is still no dramatic cell loss despite the increased severity of the model (59).

In 2001, a new double transgenic mouse model of AD expressing human mutant APP751 (carrying the Swedish and London mutations) and human mutant presenilin-1 (PS1 M146L) was reported (60). This was the first model of AD that resulted in a substantial age-related neuron loss of hippocampal pyramidal cells, which was the most dramatic in 17-month old mice (61). An important observation in this study was that the amount of plaques was not enough to explain the extent of neuron loss. Thus, another factor might contribute to the observed neuropathology in this model. Wirths et al. (62) noticed that in these mice, a considerable amount of Aβ42 in the pyramidal neurons was present, even before the formation of extracellular Aβ plaques . For this reason, Schmitz et al. (61) suggested an important role for intraneuronal Aβ in the neuropathology of AD.

In the present study, a novel double transgenic mouse model is used, carrying M233T/L235P *knocked-in* mutations in the mouse PS1 and overexpressing human APP751 bearing the London and Swedish mutations (APP/PS1 KI mice). The Aβ42:Aβ40 ratio is high in this mouse model and results of hippocampal analysis in these mice have already been published (1). A neuronal loss of 50% in the CA1/2 pyramidal cell layer was reported, which correlated with intraneuronal Aβ accumulation. This model is the first to show an age-related neuronal loss to this extent.

1.4 Aim of the current study

In this study, APP/PS1 KI mice were investigated. In these mice, the hippocampus was already extensively examined (1) and we were now interested in the frontal cortex and its potential histopathology. We analysed volume in the frontal cortex in four transgenic groups of mice: APP^{SL}, PS1He , PS1Ho and APP/PS1 KI of 2 and 10 months of age. Furthermore, the neuron numbers in the frontal cortex were determined. However, due to the lack of time, only a pilot study was performed in regard to neuron numbers.

We hypothesized that APP/PS1 KI mice show an age-related decrease in the total number of neurons in the frontal cortex. Furthermore, based on previous studies, we hypothesized that this neuron loss does not correlate with the amount of Aβ aggregates in the frontal cortex.

2 Materials and Methods

2.1 Animals

The following groups of 2-month-old (M2) and 10-month-old (M10) mice were examined: APP^{SL} mice (transgenic mice expressing human mutant APP carrying the Swedish [K670N/M671L] and London [V717I] mutations; mouse Thy-1 promoter), PS1He mice (mice expressing human PS1 mutations [M233T and L235P] knocked-in into the mouse PS1 gene in a hemizygous manner), PS1Ho mice (mice expressing human PS1 mutations [M233T and L235P] knocked-in into the mouse PS1 gene in a homozygous manner) and APP/PS1 knock-in transgenic mice (mice expressing the double APP mutation and with the PS1 mutations knocked-in into the PS1 gene in a homozygous manner).

2.2 Generation of the PS1 Mutant Knock-In Mouse Line

A PS1 knock-in mouse line was derived using a two-step mutagenesis strategy. For this purpose, a targeting vector carrying base changes in the coding region at codons M233T and L235P and surrounding introns of the PS1 gene was created (Fig.3). A detailed description of these knock-in transgenic mice has been given (1). Homozygous (Ho) mice were created and referred to as PS1Ho. For gene dosage analysis, PS1He designates the heterozygous allele. The PS1KI line was established in both pure 129SV and mixed 129SV-C57BL/6 genetic backgrounds and resulted in viable and fertile animals. The mixed PS1KI were bred with APP^{SL} mice, which overexpress human APP751 carrying the London (V717I) and Swedish (K670N/M671L) mutations under the control of the Thy1 promoter on a mixed C57BL/6-CBA genetic background (63). All animals used for this study have statistically the same genetic background: C57BL/6 50% - CBA 25% – 129SV 25%. When present, the APP transgene was heterozygote.
All experiments on animals were performed in compliance with and following the approval of the Aventis Animal Care and Use Committee, in accordance with standards for the care and use of laboratory animals (Centre National de la Recherche Scientifique-Institute of Laboratory Animal Resources) formulated by the French and European Community.

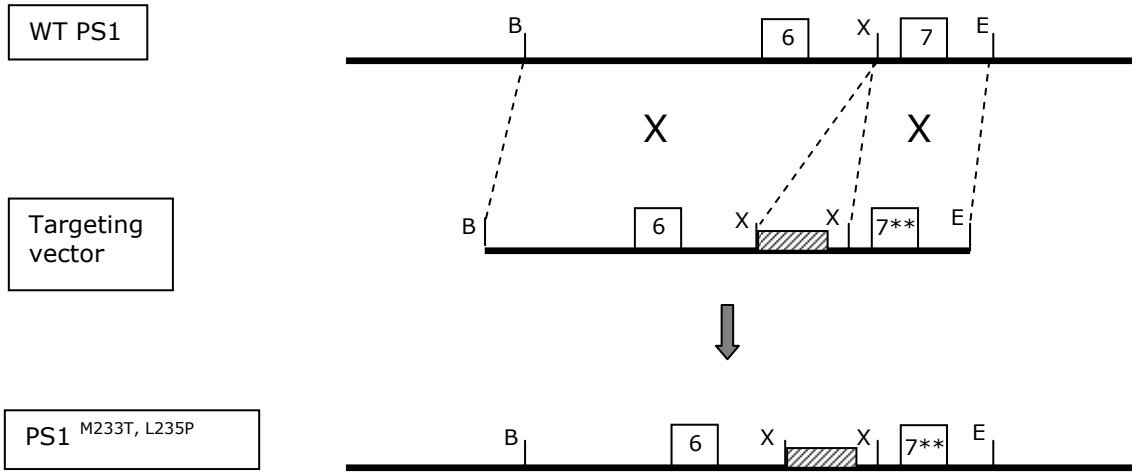

Figure 3. Gene-targeting strategy for PS1 KI mouse generation

Schematic representation of the structure and restriction map of the wild-type mouse PS1 gene (WT PS1) around Exon 7 and the targeting vector used (middle line, Targeting Vector) with the neo-cassette (striped box). Base-pair changes were carried out by directed mutagenesis to create M233T and L235P mutations (**) in Exon 7. The modified locus containing the point mutations in PS1 gene is illustrated in the lower line ($PS1^{M233T, L235T}$). Restriction enzymes: E, *EcoR*I; B, *BamH*II; X, *Xba*I.

2.3 Tissue processing

Mice were anaesthetized with chloral hydrate and transcardially perfused with tyrode followed by a fixative consisting of 4% paraformaldehyde, 15% picric acid, and 0.05% glutaraldehyde in phosphate buffer (61). Brains were removed from the skulls rapidly and the two hemispheres were separated. The right brain halves were dehydrated, paraffin embedded, cut sagitally into 4µm thick sections and were used for other analyses, which were not included in this study. The left hemi-brains were post-fixed for 2 hours at 4°C in the fixative, omitting the glutaraldehyde. Subsequently, they were cryoprotected with 30% sucrose and thereafter quickly frozen. The brains were cut frontally into series of 30µm thick sections with a cryostat (Leica, CM3050). Every tenth section was systematically assigned to one series. While cutting, the brain was divided in three regions: frontal cortex, hippocampus and cerebellum. For this study, only frontal cortex sections were analysed. For all the analyses, each time one series was selected, so that the sections were representative for the whole selected brain area. After cutting, the material was stored at -80°C until further processing.

2.4 Volume measurements of frontal cortex

Animals

For determining the frontal cortex volume of the different mouse models, the following animals were analysed: APP^{SL} mice (M2: n = 3; M10: n = 6), PS1He mice (M2: n = 4 ; M10: n = 8), PS1Ho mice (M2: n = 5; M10: n = 4) and APP/PS1 knock-in transgenic mice (M2: n = 5; M10: n = 3) (see Table 1).

Table 1. Numbers of animals used for frontal cortex volume measurements

Genotype / Age	APP^{SL}	PS1He	PS1Ho	APP/PS1 KI
M2	**3**	**4**	**5**	**5**
M10	**6**	**8**	**4**	**3**

Histochemistry

One series of every tenth frontal section each was Nissl-stained for the volume measurements and neuron countings. Sections were mounted on gelatinized glass slides, air dried and defatted with Triton X-100 (Merck, Darmstadt, Germany; 0.025%, 20 min). Subsequently, sections were stained with cresyl violet (Sigma C1791; 0.01%, 11min) as described before (61). Slides were dehydrated, cleared in xylene and coverslipped using DePeX (Klinipath, Geel, Belgium).

Stereological analysis

Frontal cortex was delineated on every section between stereotaxic bregma coordinates 1,10mm and -0,22 mm (64). Delineation with a 1,25x objective (Olympus PlanApo; NA = 0.04) was carried out with a stereology workstation and StereoInvestigator software (MicroBrightField, Williston, VT) and occurred according to the literature (64, 65) (Fig.4).

Volumes of frontal cortex were calculated from the projection area measurements and the average actual section thickness after histological processing using Cavalieri's principle (66). The actual section thickness was measured with the electronic microcator of the stereology workstation and a 40x oil objective (Olympus UplanApo; NA = 1.00). All details about the stereological analysis are extensively described by Schmitz and Hof (67).

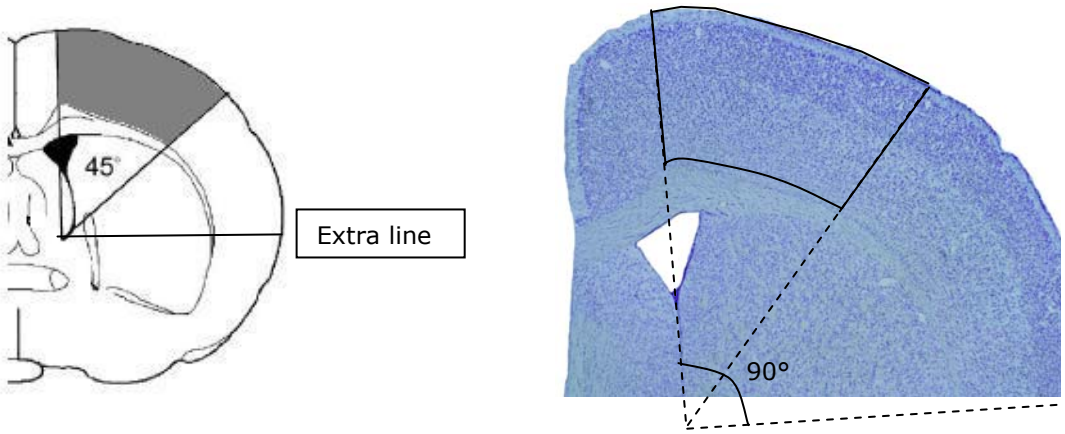

A B

Figure 4. Delineation of frontal cortex

A. Scheme depicting the region of interest: frontal cortex. Figure was adapted form Kantor et al. (65). An extra line was set at 90° for more precise delineation.

B. Representative low-power photomicrograph of 30µm thick Nissl-stained sagittal section with delineation of frontal cortex.

2.5 Neuron numbers in frontal cortex

Animals

The counting of neuron numbers in this study was due to time limitations restricted to a pilot study. Therefore, only 2-month-old and 10-month old APP/PS1 knock-in transgenic mice were analysed: M2: n = 5 and 10: n = 3 (see Table 2).

Table 2. Numbers of animals used for frontal cortex neuron numbers

Genotype / Age	APP/PS1 KI
M2	**5**
M10	**3**

Histochemistry

Neuron counts were performed on the same Nissl-stained sections that were used for volume measurements.

Stereological analysis

Left brain halves of 2- and 10-month old APP/PS1 KI mice were used to investigate the total numbers of neurons in the frontal cortex. The delineations of the volume measurements were used for cell counting. In addition, the frontal cortex was divided in two regions: layers II-III-IV and layers V-VI (Fig.5).

Total numbers of neurons were assessed by means of the Optical Fractionator and a stereological work station (StereoInvestigator, Micro Bright Field, Williston, VT). All neurons whose nucleus top came into focus within unbiased virtual counting spaces distributed in a systematic-random fashion throughout the brain region of interest were counted as described previously (68). Estimated total numbers of neurons were calculated from the number of counted neurons and the sampling probability (68).

The details of the counting procedure were as follows. Objective used for delineating the frontal cortex, layers II-III-IV and layers V-VI, 1.25x; objective used to count the neurons, 40x; base and height of the unbiased virtual counting spaces used to count neurons, 900µm and 6µm, respectively; distance between the unbiased virtual counting spaces in orthogonal directions, x = 250µm and y = 125µm; measured actual average section thickness after histological processing, 8.5 µm; average sum of unbiased virtual counting spaces used per animal, 157 for layers II-III-IV and 323 for layers V-VI ; average sum of neurons counted per animal, 392 for layers II-III-IV and 382 for layers V-VI ; average predicted coefficient of error of the estimated total numbers of neurons, 0.051 (69). Table 3 shows a summary of all details of the counting procedure.

In the Results part of this thesis, data of analysis of plaque load were also included. However, these analyses were not a part of this study and were performed by another student (unpublished data). Therefore, the analysis of plaque load will not be mentioned in the Materials and Methods.

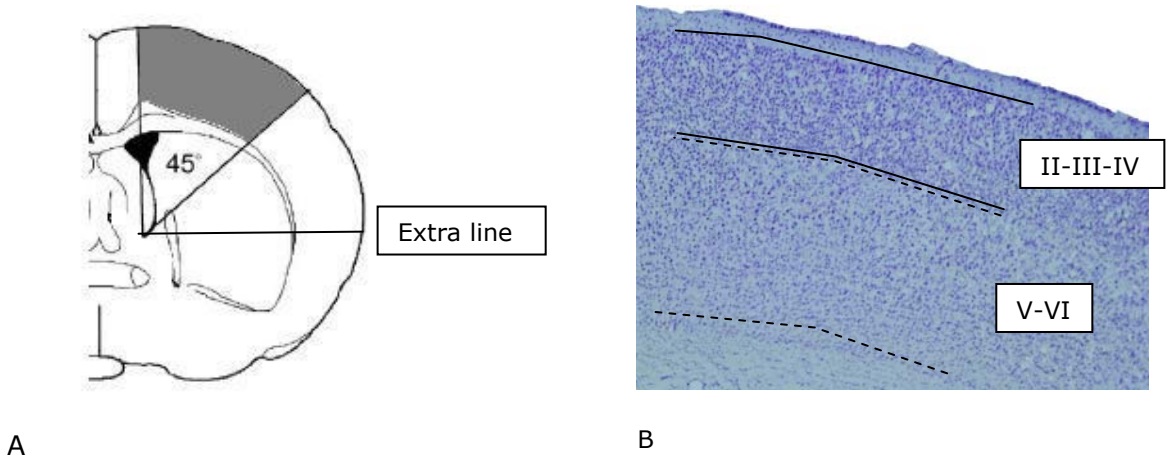

Figure 5. Delineation of frontal cortex, layers II-III-IV and layers V-VI

A. Scheme depicting the region of interest: frontal cortex. Figure was adapted from Kantor et al. (65). An extra line was set at 90° for more precise delineation.

B. Representative low-power photomicrographs of 30µm thick sagittal sections. Sections were stained with cresyl violet.

Table 3. Details of counting procedures to evaluate total numbers of neurons

Type of Neuron	Obj.	B (μm^2)	H (μm)	Dx (μm)	Dy (μm)	t (μm)	Σ OD	Σ Q^-	$CE_{pred}(\eta)$
Neurons in layers II-III-IV	40x	900	6	250	250	8.5	157	392	0.051
Neurons in layers V-VI	40x	900	6	125	125	8.5	323	382	0.051

Obj., objective used; B and H, base and height of the counting frames; D, distance between the optical disectors in orthogonal directions x and y; t, measured actual average section thickness after histologic processing; Σ OD, average sum of counting frames per animal; Σ Q^-, average number of neurons counted per animal; CE_{pred} [η], average predicted coefficient of error of the estimated total numbers of neurons using the predictions method described by (69).

2.6 Statistics

For all groups of mice, mean and standard error of the mean (SEM) were calculated for all investigated variables (volume and neuron number).

For the volume measurements, comparisons between the groups were performed with two-way analysis of variance (two-way ANOVA; four genotypes and two age groups per genotype) followed by post-hoc Bonferroni multiple comparison tests for pair-wise comparisons.

For neuron numbers and volume measurements of the APP/PS1 KI mice at two ages (as well as plaque load, data not shown), unpaired t-tests were performed.

Statistical significance was established at $P<0.05$. All calculations were performed using GraphPad Prism (Version 4.00 for Windows; GraphPad Software, San Diego, CA).

2.7 Photomicrography

Photomicrographs shown in Fig.4, 5, 13 and 14 were produced by digital photography using an Olympus DP 70 digital camera attached to an Olympus AX 70 microscope and cell^P software Version 2.3 (Soft Imaging System, Münster, Germany). In case of Figure 14, photomicrographs were deconvoluted with AutoDeblur software Version 9.3 (Autoquant Imaging, Watervliet, NY, USA) (two iteration steps). The final figures were constructed using Corel Photo-Paint v.11 and Corel Draw v.11 (Corel, Ottawa, Canada). Only minor adjustments of contrast and brightness were made, without altering the appearance of the original materials.

3 Results

3.1 Volume measurements of frontal cortex

Volume measurements were carried out on the frontal cortex of APP^{SL} , PS1He, PS1Ho and APP/PS1 KI mice. Two-way ANOVA with Bonferroni posthoc tests indicated no significant age or genotype differences between the groups in regard to frontal cortex volume. However, the volume seemed to decrease to some extent between the 2-month old and 10-month old APP/PS1 KI mice (Fig.6). It was therefore decided to do further analyses on these two groups of mice.

The frontal cortex of 2-month old and 10-month old APP/PS1 KI mice was divided in two regions: layers II-III-IV and layers V-VI (see Materials and Methods for details). Unpaired t-tests did not show a significant difference between the ages of APP/PS1 KI mice both in layers II-III-IV (Fig.7) as well as layers V-VI (Fig.8). However, there was a tendency in layers V-VI towards a decreased volume (P-value of 0.069).

In conclusion, there were no significant differences in volume measurements between the different ages and genotypes of APP^{SL}, PS1He, PS1Ho and APP/PS1 KI mice.

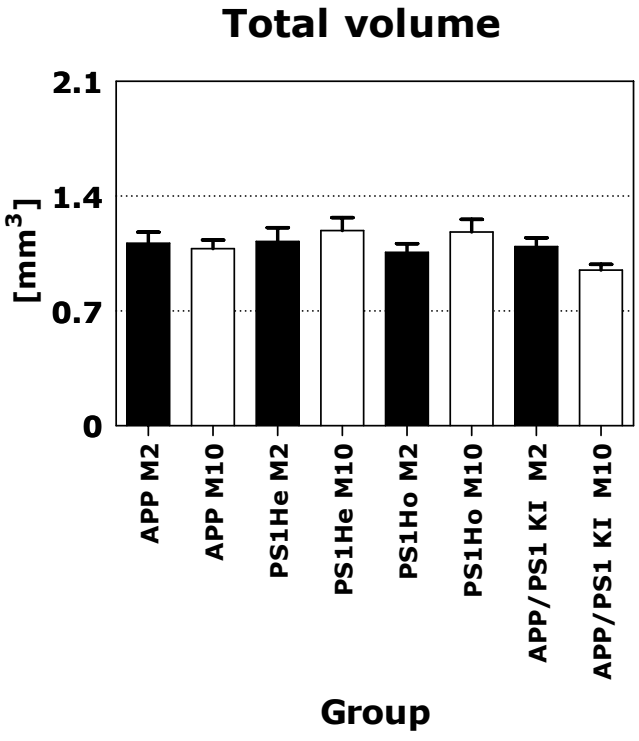

Figure 6. Results of stereological analysis of frontal cortex volume

Stereological assessment of volumes of frontal cortex of APP^{SL}, PS1He, PS1Ho and APP/PS1 KI mice. Of each transgenic group, 2-month old and 10-month old animals were analysed. Differences between groups were tested with two-way analysis of variance, followed by posthoc Bonferroni's multiple comparison test for pair-wise comparisons. A P-value of <0.05 was considered statistically significant.

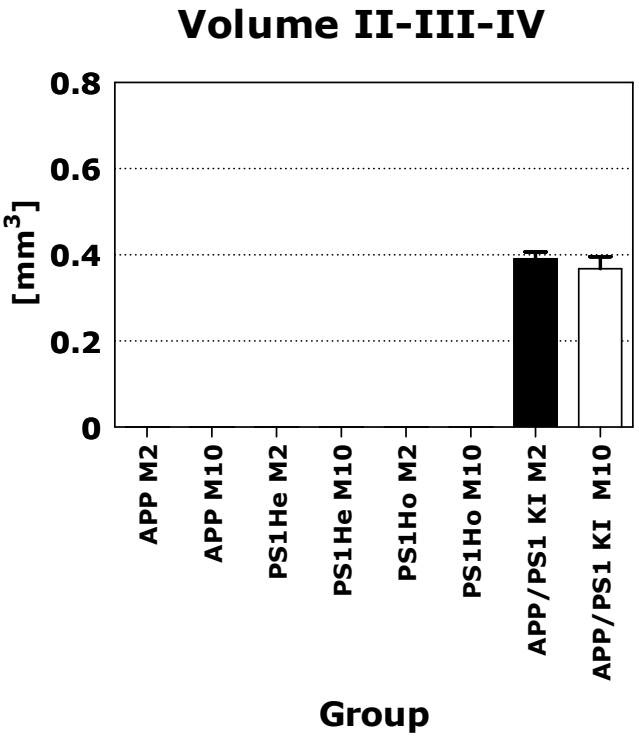

Figure 7. Results of stereological analysis of frontal cortex volume of layers II-III-IV

Stereological assessment of volumes of layers II-III-IV of frontal cortex of 2- and 10-month old APP/PS1 KI mice. Differences between groups were tested with an unpaired t-test. A P-value of <0.05 was considered statistically significant.

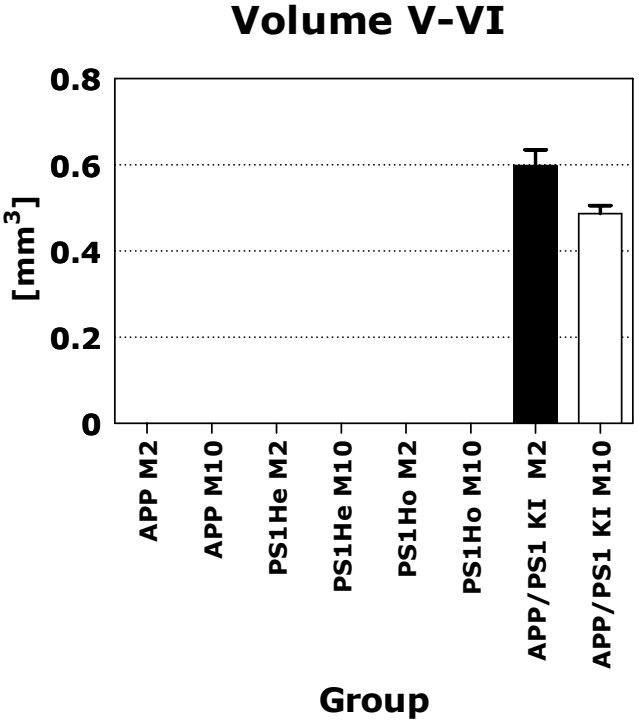

Figure 8. Results of stereological analysis of frontal cortex volume of layers V-VI

Stereological assessment of volumes of layers V-VI of frontal cortex of 2- and 10-month old APP/PS1 KI mice. Differences between groups were tested with an unpaired t-test. A P-value of <0.05 was considered statistically significant.

3.2 Neuron numbers in frontal cortex

Neuron numbers of the frontal cortex were obtained with stereological analysis in 2-month old and 10-month old APP/PS1 KI mice. Again, the frontal cortex was subdivided in two regions (layers II-III-IV and V-VI), which were analysed separately.

Statistical analysis was performed using unpaired t-tests. In layers II-III-IV, there was no significant difference between the 2-month old and 10-month old APP/PS1 KI mice (Fig.9). On the contrary, in layers V-VI a significant decrease of neurons in the 10-month old APP/PS1 KI mice compared to the 2-month old ($P<0.05$) was observed (Fig.10). The average decrease was 28%.

From the analysis of plaque load, it became apparent that the plaque load increased with age when comparing 2-month old and 10-month old APP/PS1 KI mice. Performing unpaired t-test, the differences between the 2-month old and 10-month old APP/PS1 KI mice were significant in layers II-III-IV (Fig.11) as well as layers V-VI (Fig.12). The plaque load analyses were not part of this study, however the results were included in order to explain the neuron loss observed in layers V-VI of 10-month old APP/PS1 KI mice (unpublished data; see Discussion). The plaque load in layers II-III-IV increased from 0,2% in 2-month old to 7,2% in 10-month old APP/PS1 KI mice (Fig.11). In layers V-VI, 2-month old APP/PS1 KI mice had a plaque load of 0,9% that increased to 11% in 10-month old APP/PS1 KI mice (Fig.12). In Figure 13, representative pictures are depicted showing the plaque load in a 10-month old APP/PS1 KI mouse. The amyloid plaques were principally observed in layers V-VI of the frontal cortex and the increase of plaque load with age was clearly visible (not shown). Another observation was the presence of neurons in the frontal cortex that contained intraneuronal fibrillar Aβ, visualized with a Thioflavine S-staining (Fig.14).

Hence, in 10-month old APP/PS1 KI mice a neuron loss of 28% was observed located in layers V-VI of the frontal cortex. Furthermore, the APP/PS1 KI mice had a plaque load in the frontal cortex that significantly increased with age.

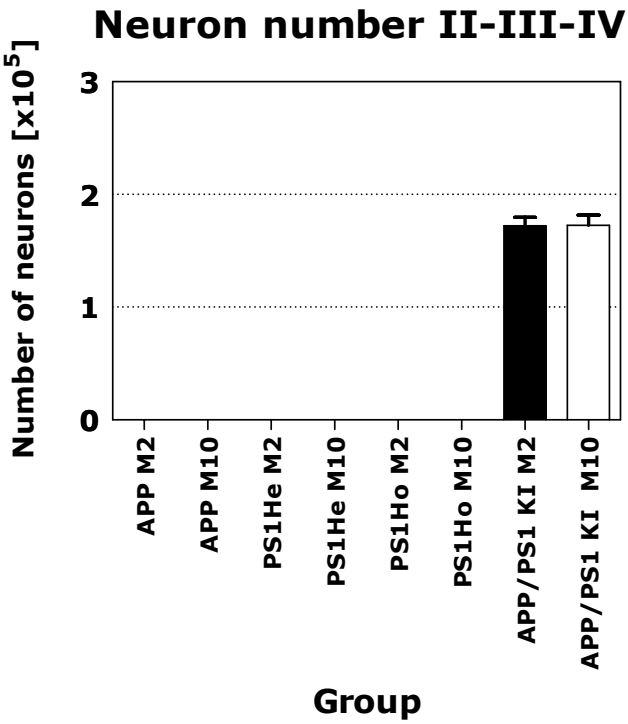

Figure 9. Results of stereological analysis of neuron numbers in layers II-III-IV of frontal cortex

Layers II-III-IV of the frontal cortex of 2-month-old and 10-month-old APP/PS1 KI mice were analysed by high precision design-based stereology (see Materials and Methods for details). Differences between these groups were assessed with an unpaired t-test. Statistical significance was established at $P < 0.05$.

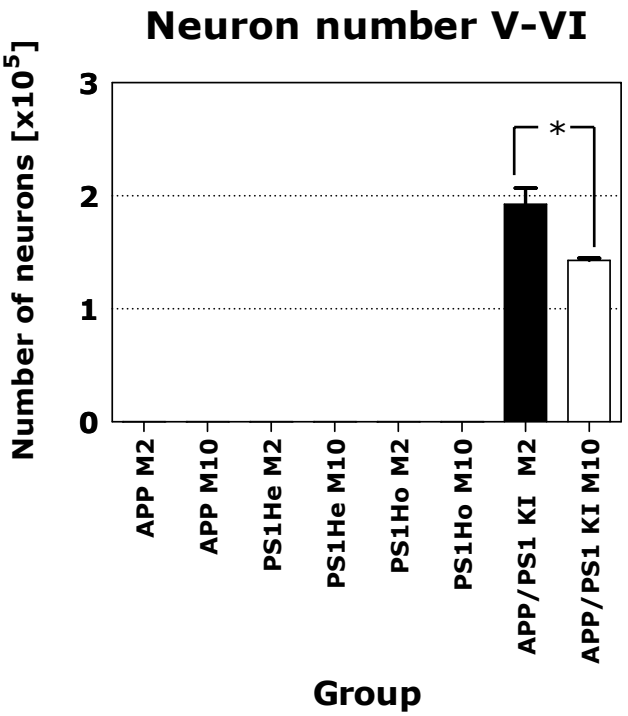

Figure 10. Results of stereological analysis of neuron numbers in layers II-III-IV of frontal cortex

Layers V-VI of the frontal cortex of 2-month-old and 10-month-old APP/PS1 KI mice were analysed by high precision design-based stereology (see Materials and Methods for details). Differences between these groups were assessed with an unpaired t-test. Statistical significance was established at $P < 0.05$, *.

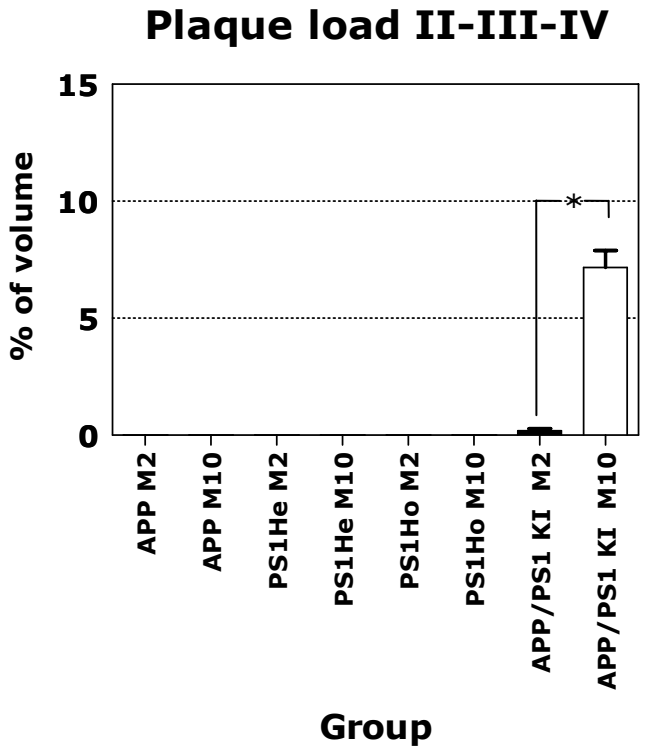

Figure 11. Percentage of frontal cortex layers II-III-IV occupied by plaques

Plaques in layers II-III-IV of frontal cortex in 2-month old and 10-month old APP/PS1 KI mice were counted by point-counting methods. Differences were statistically analysed by an unpaired t-test and significance was set at P-value < 0.05, *.

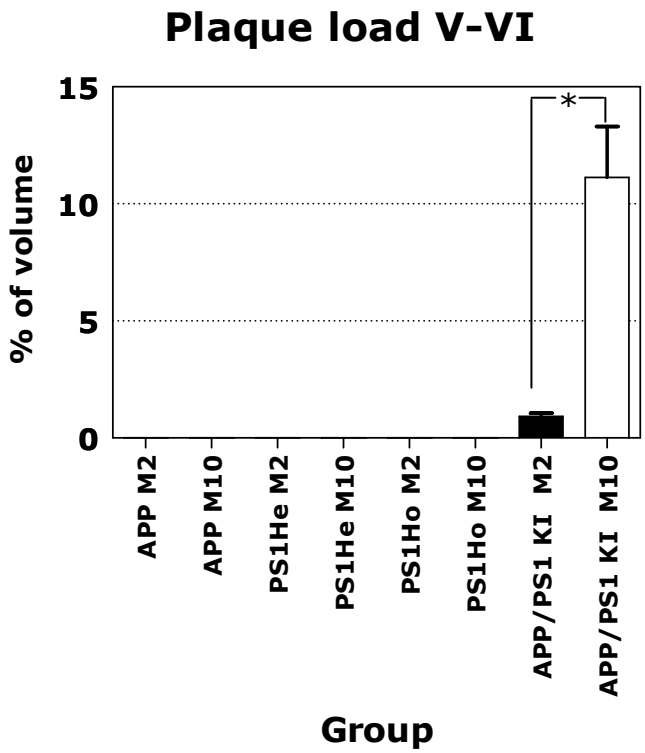

Figure 12. Percentage of frontal cortex layers V-VI occupied by plaques

Plaques in layers V-VI of frontal cortex in 2-month old and 10-month old APP/PS1 KI mice were counted by point-counting methods. Differences were statistically analysed by an unpaired t-test and significance was set at P-value < 0.05, *.

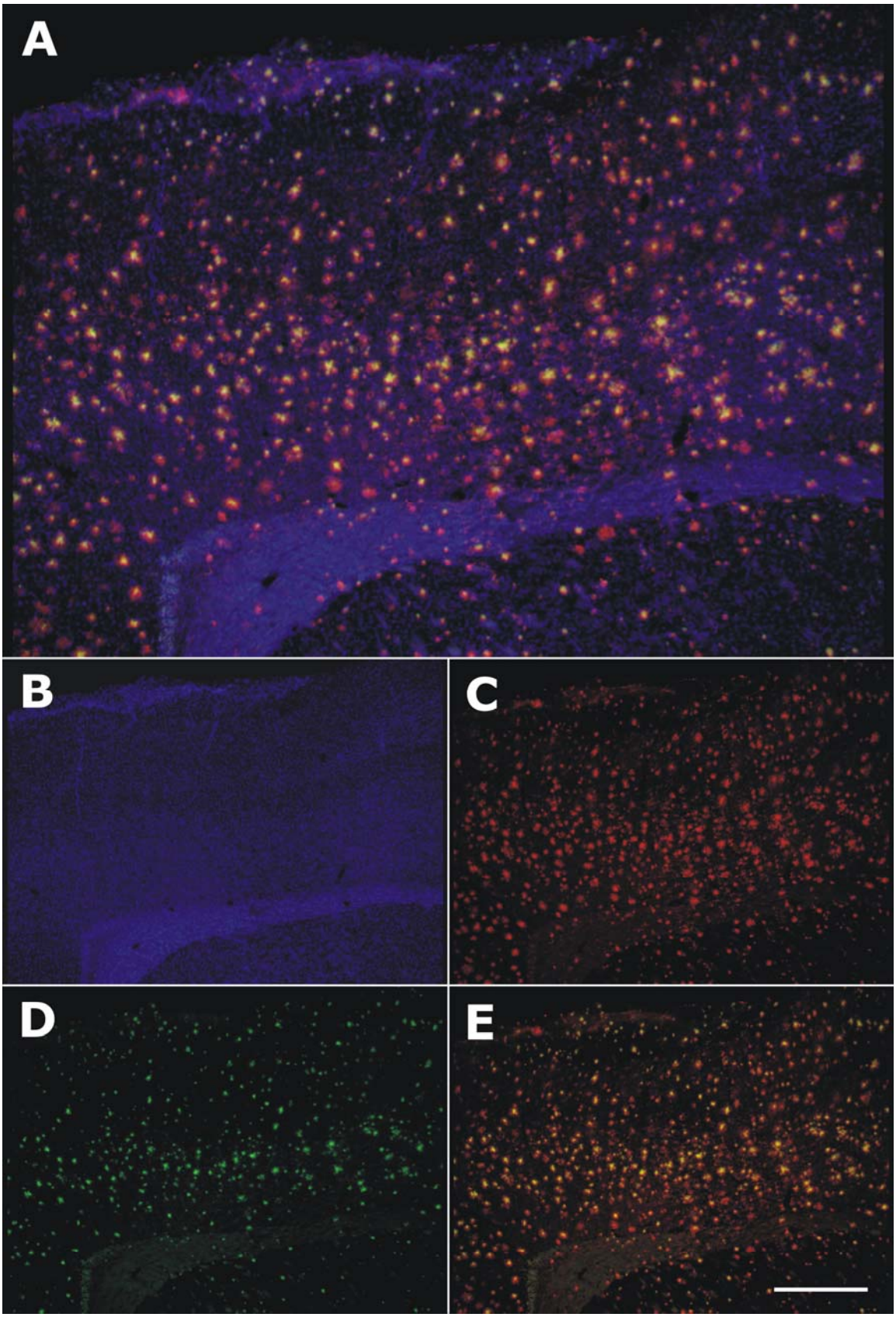

Figure 13. Plaque load in frontal cortex of 10-month old APP/PS1 KI mice

Representative low-power photomicrographs of a Hoechst [blue,(B)], Aβ [red,(C)] and Thioflavine S [green,(D)] triple staining in the frontal cortex of a 10-month old APP/PS1 KI mouse [merged in (A)]. Note the presence of plaques predominantly in layers V-VI of the frontal cortex. (E) shows both Aβ and Thioflavine S. Note the Thioflavine S-positive fibrillar deposits that are part of the Aβ plaques. Scale bar = 500 µm in (A) and 1mm in (B) to (E).

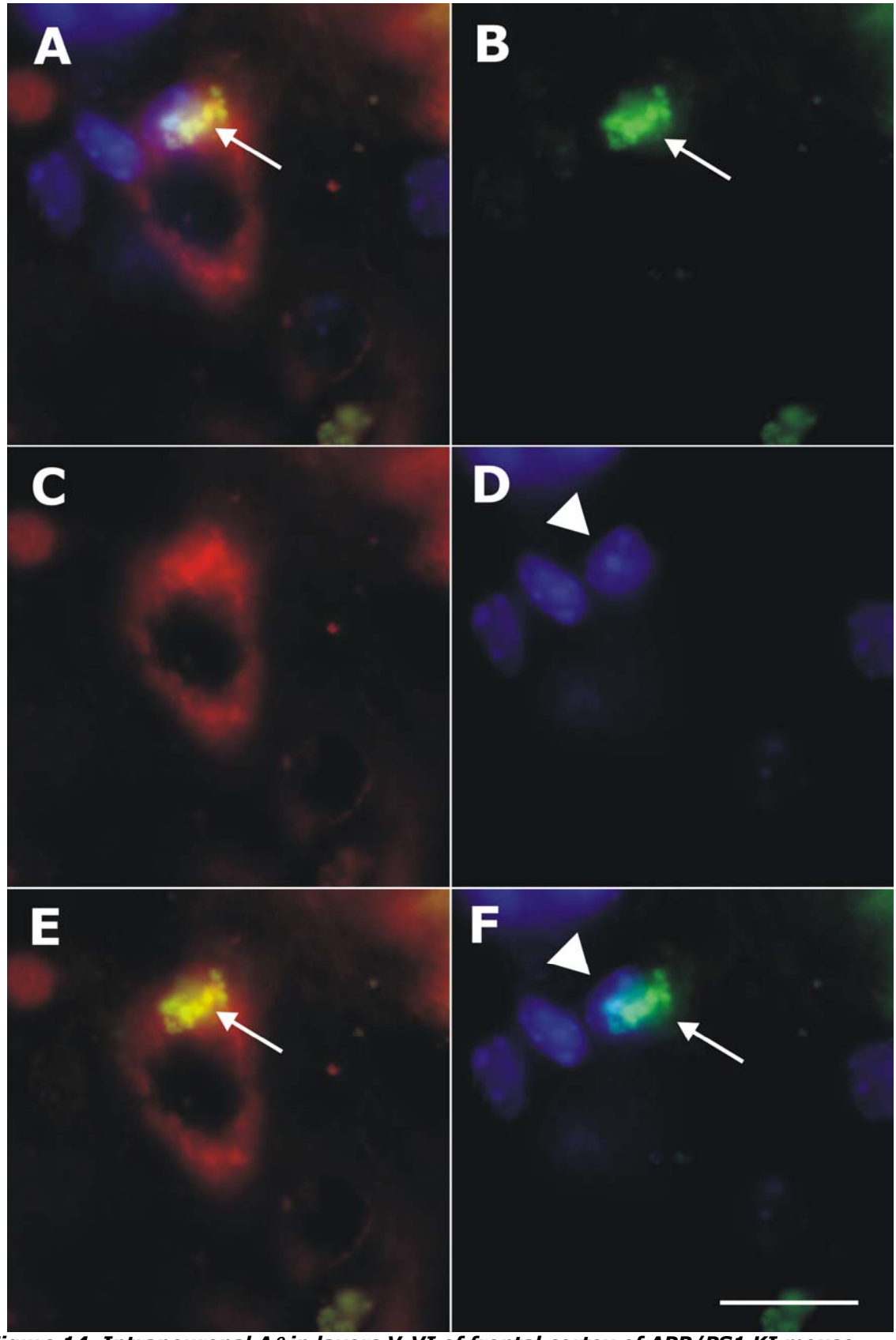

Figure 14. Intraneuronal Aβ in layers V-VI of frontal cortex of APP/PS1 KI mouse

Representative high-power photomicrographs of a Thioflavine S [green,(B)], Aβ [red,(C)] and Hoechst [blue,(D)] triple staining in the frontal cortex layers V-VI of a 10-month old APP/PS1 KI mouse [merged in (A)]. (E) shows both Aβ and Thioflavine S. Note the colocalization of intraneuronal Aβ and Thioflavine S (arrow). (F) shows both Hoechst and Thioflavine S. Thioflavine S is not present in the glial cell (arrowhead) located near the pyramidal neuron. Scale bar = 20 μm.

4 Discussion

In the present study, the frontal cortex of different mouse models of AD was investigated. The frontal cortex volume was assessed in 2- and 10-month old APP^{SL}, PS1He, PS1Ho and APP/PS1 KI mice. No significant differences were detected with respect to the genotypes and ages (Fig.6). However, a tendency towards a decreased frontal cortex volume between 2- and 10-month old APP/PS1 KI mice was found. Based on these results, a pilot study assessing neuron numbers in the frontal cortex was performed in these mice. Cortical layers II-III-IV did not show any significant differences in total numbers of neurons when comparing both age groups (Fig.9). Nonetheless, in layers V-VI a significantly decreased number of neurons was present in 10-month old APP/PS1 KI mice compared to 2-month old (Fig.10).

Focusing on amyloid burden, the plaque load was determined in layers II-III-IV and layers V-VI of frontal cortex of 2-month old and 10-month old APP/PS1 KI mice. The 10-month old mice showed a significant increase in plaque load in layers II-III-IV and layers V-VI of the frontal cortex (Fig.11,12). An average plaque load of 7,2% in layers II-III-IV and 11% in layers V-VI of frontal cortex in 10-month old APP/PS1 KI mice was established. However, the average plaque load (11%) in layers V-VI of the 10-month old APP/PS1 KI mice cannot fully account for the reported 28% neuron loss in the same area. Based on previous literature and our observation of intraneuronal Aβ deposits present in layers V-VI neurons of 10-month old APP/PS1 KI frontal cortex (Fig.13,14), we suggest that intraneuronal Aβ accumulation might contribute to the observed neuron loss in this mouse model.

4.1 First report of substantial cortical neuron loss in a transgenic mouse model of AD

This study describes a neuron loss of 28% in layers V-VI of the frontal cortex of APP/PS1 KI mice and is hereby the first report of a substantial neuron loss is the frontal cortex of transgenic mice. With respect to the hippocampus, several transgenic mouse models have been developed showing neuron loss. In APP23 mice, a mild (14%) neuron loss in CA1 of the hippocampus was reported (54). Yet, no neuron loss was detected in the cortex of these mice. In 2004, Schmitz et al. (61) reported a substantial decrease of pyramidal neurons in 17-month old double transgenic $APP^{751}/PS1^{M146L}$ mice. However, the most severe neuron loss in hippocampus was described in APP/PS1 KI mice (1). Already at 10 months of age, these mice showed over 50% neuron loss in the pyramidal layer of hippocampal CA1/2 region. Therefore, the results of the neuron loss in the frontal cortex of the APP/PS1 KI mice are in line with the literature.

The investigation of both the volume and neuron number of frontal cortex was done by high precision design-based stereology. This technique allows the accurate estimate of neuron numbers within specific brain regions without relying on density measurements that can be confounded by changes of neuronal size or size of the region of interest (67). Therefore, this method is appropriate for cell counting and the observed neuron loss can be considered a valid result.

4.2 Plaque load is not the sole cause of neuron loss

The average plaque load was determined using a double staining for Aβ and Thioflavine S. The average plaque load in layers V-VI of the frontal cortex of 10-month old APP/PS1 KI mice was 11%. On the contrary, the observed neuron loss in the investigated brain area was higher (28%). Therefore, the majority of the reported neuron loss can not be attributed to extracellular Aβ deposits.

Urbanc et al. (26) proposed several mechanisms by which amyloid plaques can influence the surrounding pyramidal neurons. From the present study, we can conclude that plaques do not only displace the neurons. If that was the case, the neuron number would have been equal in both 2-month old and 10-month old APP/PS1 KI mice. It seems that another mechanism is applicable here, namely that either the amyloid deposit is toxic for the neurons located within the plaque or that the plaque kills the neurons located both within and around it. Based on the observation in this study of a higher neuron loss as compared to the plaque load, the latter mechanism is most probably present in the APP/PS1 KI mice.

The poor relationship between plaque load and neuron loss fits with previous studies, performed both on human *post-mortem* tissue and transgenic mouse models.

Gomez-Isla et al. (34) have insinuated a lack of correlation between neuronal loss and extent of the plaque load present in the human AD brain. Furthermore, the $APP^{751}/PS1^{M146L}$ transgenic mouse model developed a substantial neuron loss (25-30%) in the pyramidal cell layer of the hippocampus by the age of 17 months. In these mice, the amyloid plaque burden did not account fully for the neuronal loss (61).

On the contrary, in APP23 mice, a mild neuron loss was reported in the hippocampus that correlated well with the amount of extracellular Aβ deposits (54). However, as in this study both homozygous and hemizygous mice were included in the calculations for this correlation between plaque load and neuron loss (and the hemizygous mice showed almost no plaques), it is possible that there was a neutralization effect present.

These findings imply the existence of another component that might contribute to the observed neuron loss in APP/PS1 KI mice. Until this day, no other mouse models have been developed showing neuron loss in the frontal cortex.

4.3 Intraneuronal Aβ: a possible key player in the Aβ cascade hypothesis?

Since the plaque load in APP/PS1 KI mice is not responsible for the entire observed neuron loss in the frontal cortex and taking the present literature into account, it is likely that the intraneuronal Aβ aggregates are a contributing factor in neurodegeneration. In other words, at least a part of the observed neuron loss might be caused by the intracellular Aβ, independent of extracellular Aβ deposits.

Indeed, intraneuronal Aβ as well as Thioflavine S-positive deposits have been identified in neurons of frontal cortex layers V-VI of 10-month old APP/PS1 KI mice (Fig.13,14).
The causative link between neuron loss and intraneuronal Aβ accumulation was already suggested in the APP/PS1 KI mouse model, based on findings in the hippocampus (1). In APP/PS1 KI mice, Casas et al. (2004) observed a substantial accumulation of intraneuronal Aβ in the hippocampus starting at 2 months of age. In addition, they also showed a loss of neurons in this region. Moreover, a clear colocalization of intraneuronal Aβ and Thioflavine S was observed in pyramidal neurons of the hippocampus, implicating that at least some of the intraneuronal Aβ was present in the fibrillar form (1). This is in line with our study, in which we found intraneuronal Aβ and Thioflavine S colocalization in layers V-VI of the frontal cortex, the region of the observed neuron loss (Fig.13,14). The close relationship between intraneuronal Aβ, Thioflavine S and neuron loss suggests a causative role for these components in the neuropathology seen in AD. The present study therefore supports the previous finding in this model and strengthens the detrimental role of intraneuronal Aβ for the neuronal survival in AD brains.

In addition, the literature contains several reports of the neurotoxicity of intraneuronal Aβ accumulation. The concept of the early pathology induced by intraneuronal Aβ (70) associates well with the study of Lee et al. (71) indicating the occurrence of synaptic, axonal and dendritic injury in early AD. Furthermore, various publications have showed the involvement of neuronal Aβ in neuron death in AD (26, 61).
In human AD, the neuronal loss can go up to 50% in vulnerable regions of the cortex. However, several studies showed that the amount of extracellular Aβ deposits has little or no correlation with this neuron loss (34, 72). Moreover, the severity of AD could not be predicted by the amount of amyloid plaques present in the brain (73). Finally, from human *post-mortem* tissue, it has been concluded that neuronal toxicity in AD is mainly associated with Thioflavine S-positive deposits (26).
Additionally, numerous transgenic mouse models showing an considerable high plaque load in the brain revealed no neuron loss (43, 59). Schmitz et al. (61) clearly stated that in the $APP^{751}/PS1^{M146L}$ mouse model the neuron loss exceeded the plaque load.

4.4 Aβ42 as the most malignant Aβ variant

Casas et al. (1) reported a elevated Aβ42:Aβtotal ratio in APP/PS1 KI mice and a high amount of N-truncated forms of Aβ42 compared to APP^{SL} mice. These features are far more similar to the human AD brain compared to other developed mouse models, including APP^{SL} mice.
Several reports have been made about the neurotoxicity of Aβ42. Aβ42 is more neurotoxic for cultured neurons *in vitro* than Aβ40 (74). Other *in vitro* studies show that Aβ42 solution form soluble oligomers much more rapidly than Aβ40. Furthermore, these Aβ42 solutions are more harmful for neuroblastoma cells than Aβ40 solutions. This effect might possibly be mediated by

the soluble oligomers formed by Aβ42 (75). According to McLean et al. (76), the soluble pool correlates better with the severity of the pathology seen in AD brains than the extracellular Aβ deposits. The soluble Aβ, both intracellular and extracellular, can contribute to neurodegeneration (77). In addition, a recent study of Billings et al. (78), reported the relationship between intraneuronal Aβ accumulation and cognitive decline in a triple transgenic APP/PS1/tau mouse model.

Considering the relative higher amount of Aβ42 in APP/PS1 KI mice, it is reasonable to presume that these toxic components attribute to the neuron loss seen in the frontal cortex. This suggestion is supported by the observation that intraneuronal Aβ42 is present in pyramidal neurons even before the formation of extracellular Aβ deposits (60).
Because Aβ42 is the most toxic form of Aβ and this form has the highest relative concentration in the APP/PS1 KI mice, one could assume that the amount of Aβ42 is a predictive factor for the extent of the neuron loss. In other words, intraneuronal accumulation of Aβ seems to be a key, possibly preventable, step in the pathogenesis of AD.

4.5 Presenilin as a modifying gene

Various transgenic mouse models of AD have been developed over the years, using mostly FAD-associated mutations in APP. These transgenic mice are important *in vivo* models for determining the pathogenesis in AD brains and which genes play a possible role in this. Several models have shown AD-like pathology such as amyloid plaques, synaptic dysfunction and cognitive impairments (39). However, only a few models developed neurodegeneration and as a consequence, the exact link between amyloidogenesis and neuron loss is not established yet. Two recent mouse models have shown a substantial age-related neuron loss: 1) $APP^{751}/PS1^{M1146L}$ mice with a double mutation in APP and a mutation in PS1 and 2) APP/PS1 KI mice with the double Swedish and London mutation in APP and M233T and L235P mutations knocked into the PS1 gene. A 35% neuron loss in the CA1/2 region of the hippocampus of $APP^{751}/PS1^{M146L}$ mice was reported by Schmitz et al. (61). The importance of this mouse model was underlined by Dickson (79). However, APP/PS1 KI mice show the most dramatic neuron loss in the CA1/2 region of hippocampus (1). In the same study, Casas et al. reported no neuron loss in the hippocampus of APP^{SL} mice and therefore concluded that the expression of mutant APP is not a guarantee for neurotoxicity.
Based on the previous findings in these two mouse models of AD, in addition to the reported neuron loss the frontal of APP/PS1 KI mice in this study, the modifying role of PS1 in transgenic mouse models of AD is supported.

4.6 General conclusion

The APP/PS1 KI mouse model is the first transgenic mouse model of AD that shows a substantial early onset age-related neuron loss in the frontal cortex, which is independent of plaque burden. Investigating this mouse model, the roles of intracellular and extracellular Aβ could be clarified and the mechanisms of neuron loss *in vivo* in different brain regions could be elucidated. Furthermore, the APP/PS1 KI mouse model is so far the model that represents the most similarities with human AD and can therefore be used for testing possible therapeutics. This mouse model provides an excellent framework to pinpoint detrimental mechanisms involved in neurodegeneration in AD.

5 References

1. Casas C, Sergeant N, Itier JM, Blanchard V, Wirths O, van der Kolk N, et al. Massive CA1/2 neuronal loss with intraneuronal and N-terminal truncated Abeta42 accumulation in a novel Alzheimer transgenic model. Am J Pathol. 2004 Oct;165(4):1289-300.
2. Alzheimer A. Ubereine eigenartige Erkrankung der Hirnrinde. [A peculiar disease of the cerebral cortex.]. Allg Z Psychiatr-Gerichtl Med. 1907;64:146-8.
3. Dickson DW. Neuropathology of Alzheimer's disease and other dementias. Clin Geriatr Med. 2001 May;17(2):209-28.
4. Probst A, Langui D, Ulrich J. Alzheimer's disease: a description of the structural lesions. Brain Pathol. 1991 Jul;1(4):229-39.
5. Peskind ER. Neurobiology of Alzheimer's disease. J Clin Psychiatry. 1996;57 Suppl 14:5-8.
6. Faber-Langendoen K, Morris JC, Knesevich JW, LaBarge E, Miller JP, Berg L. Aphasia in senile dementia of the Alzheimer type. Ann Neurol. 1988 Apr;23(4):365-70.
7. Rubin EH, Morris JC, Storandt M, Berg L. Behavioral changes in patients with mild senile dementia of the Alzheimer's type. Psychiatry Res. 1987 May;21(1):55-62.
8. Mayeux R. Epidemiology of neurodegeneration. Annu Rev Neurosci. 2003;26:81-104.
9. Helmer C, Joly P, Letenneur L, Commenges D, Dartigues JF. Mortality with dementia: results from a French prospective community-based cohort. Am J Epidemiol. 2001 Oct 1;154(7):642-8.
10. Cummings JL, Cole G. Alzheimer disease. Jama. 2002 May 8;287(18):2335-8.
11. Tanzi RE, McClatchey AI, Lamperti ED, Villa-Komaroff L, Gusella JF, Neve RL. Protease inhibitor domain encoded by an amyloid protein precursor mRNA associated with Alzheimer's disease. Nature. 1988 Feb 11;331(6156):528-30.
12. Levy-Lahad E, Wasco W, Poorkaj P, Romano DM, Oshima J, Pettingell WH, et al. Candidate gene for the chromosome 1 familial Alzheimer's disease locus. Science. 1995 Aug 18;269(5226):973-7.
13. Holmes C. Genotype and phenotype in Alzheimer's disease. Br J Psychiatry. 2002 Feb;180:131-4.
14. Saunders AM, Strittmatter WJ, Schmechel D, George-Hyslop PH, Pericak-Vance MA, Joo SH, et al. Association of apolipoprotein E allele epsilon 4 with late-onset familial and sporadic Alzheimer's disease. Neurology. 1993 Aug;43(8):1467-72.
15. Ferri CP, Prince M, Brayne C, Brodaty H, Fratiglioni L, Ganguli M, et al. Global prevalence of dementia: a Delphi consensus study. Lancet. 2005 Dec 17;366(9503):2112-7.
16. Ott A, Breteler MM, van Harskamp F, Claus JJ, van der Cammen TJ, Grobbee DE, et al. Prevalence of Alzheimer's disease and vascular dementia: association with education. The Rotterdam study. Bmj. 1995 Apr 15;310(6985):970-3.
17. Citron M, Westaway D, Xia W, Carlson G, Diehl T, Levesque G, et al. Mutant presenilins of Alzheimer's disease increase production of 42-residue amyloid beta-protein in both transfected cells and transgenic mice. Nat Med. 1997 Jan;3(1):67-72.
18. Hardy J, Selkoe DJ. The amyloid hypothesis of Alzheimer's disease: progress and problems on the road to therapeutics. Science. 2002 Jul 19;297(5580):353-6.
19. Tanzi RE, Bertram L. Twenty years of the Alzheimer's disease amyloid hypothesis: a genetic perspective. Cell. 2005 Feb 25;120(4):545-55.
20. Koo EH. The beta-amyloid precursor protein (APP) and Alzheimer's disease: does the tail wag the dog? Traffic. 2002 Nov;3(11):763-70.
21. Slunt HH, Thinakaran G, Von Koch C, Lo AC, Tanzi RE, Sisodia SS. Expression of a ubiquitous, cross-reactive homologue of the mouse beta-amyloid precursor protein (APP). J Biol Chem. 1994 Jan 28;269(4):2637-44.
22. Lammich S, Kojro E, Postina R, Gilbert S, Pfeiffer R, Jasionowski M, et al. Constitutive and regulated alpha-secretase cleavage of Alzheimer's amyloid precursor protein by a disintegrin metalloprotease. Proc Natl Acad Sci U S A. 1999 Mar 30;96(7):3922-7.
23. Citron M, Diehl TS, Gordon G, Biere AL, Seubert P, Selkoe DJ. Evidence that the 42- and 40-amino acid forms of amyloid beta protein are generated from the beta-amyloid precursor protein by different protease activities. Proc Natl Acad Sci U S A. 1996 Nov 12;93(23):13170-5.
24. Seubert P, Oltersdorf T, Lee MG, Barbour R, Blomquist C, Davis DL, et al. Secretion of beta-amyloid precursor protein cleaved at the amino terminus of the beta-amyloid peptide. Nature. 1993 Jan 21;361(6409):260-3.
25. Mullan M, Crawford F, Axelman K, Houlden H, Lilius L, Winblad B, et al. A pathogenic mutation for probable Alzheimer's disease in the APP gene at the N-terminus of beta-amyloid. Nat Genet. 1992 Aug;1(5):345-7.
26. Urbanc B, Cruz L, Le R, Sanders J, Ashe KH, Duff K, et al. Neurotoxic effects of thioflavin S-positive amyloid deposits in transgenic mice and Alzheimer's disease. Proc Natl Acad Sci U S A. 2002 Oct 29;99(22):13990-5.
27. Braak H, Braak E, Yilmazer D, de Vos RA, Jansen EN, Bohl J. Pattern of brain destruction in Parkinson's and Alzheimer's diseases. J Neural Transm. 1996;103(4):455-90.
28. Price DL, Sisodia SS. Mutant genes in familial Alzheimer's disease and transgenic models. Annu Rev Neurosci. 1998;21:479-505.
29. Morrison JH, Hof PR. Selective vulnerability of corticocortical and hippocampal circuits in aging and Alzheimer's disease. Prog Brain Res. 2002;136:467-86.
30. Broadbent NJ, Squire LR, Clark RE. Spatial memory, recognition memory, and the hippocampus. Proc Natl Acad Sci U S A. 2004 Oct 5;101(40):14515-20.

31. Miller EK, Cohen JD. An integrative theory of prefrontal cortex function. Annu Rev Neurosci. 2001;24:167-202.
32. Mann DM, Marcyniuk B, Yates PO, Neary D, Snowden JS. The progression of the pathological changes of Alzheimer's disease in frontal and temporal neocortex examined both at biopsy and at autopsy. Neuropathol Appl Neurobiol. 1988 May-Jun;14(3):177-95.
33. Mesulam MM, Geula C. Acetylcholinesterase-rich pyramidal neurons in the human neocortex and hippocampus: absence at birth, development during the life span, and dissolution in Alzheimer's disease. Ann Neurol. 1988 Dec;24(6):765-73.
34. Gomez-Isla T, Hollister R, West H, Mui S, Growdon JH, Petersen RC, et al. Neuronal loss correlates with but exceeds neurofibrillary tangles in Alzheimer's disease. Ann Neurol. 1997 Jan;41(1):17-24.
35. De Souza EB, Whitehouse PJ, Kuhar MJ, Price DL, Vale WW. Reciprocal changes in corticotropin-releasing factor (CRF)-like immunoreactivity and CRF receptors in cerebral cortex of Alzheimer's disease. Nature. 1986 Feb 13-19;319(6054):593-5.
36. Morrison JH, Hof PR. Life and death of neurons in the aging brain. Science. 1997 Oct 17;278(5337):412-9.
37. Bussiere T, Giannakopoulos P, Bouras C, Perl DP, Morrison JH, Hof PR. Progressive degeneration of nonphosphorylated neurofilament protein-enriched pyramidal neurons predicts cognitive impairment in Alzheimer's disease: stereologic analysis of prefrontal cortex area 9. J Comp Neurol. 2003 Aug 25;463(3):281-302.
38. Bloom FE, Reilly JF, Redwine JM, Wu CC, Young WG, Morrison JH. Mouse models of human neurodegenerative disorders: requirements for medication development. Arch Neurol. 2005 Feb;62(2):185-7.
39. Spires TL, Hyman BT. Transgenic models of Alzheimer's disease: learning from animals. NeuroRx. 2005 Jul;2(3):423-37.
40. Zheng H, Jiang M, Trumbauer ME, Sirinathsinghji DJ, Hopkins R, Smith DW, et al. beta-Amyloid precursor protein-deficient mice show reactive gliosis and decreased locomotor activity. Cell. 1995 May 19;81(4):525-31.
41. Shen J, Bronson RT, Chen DF, Xia W, Selkoe DJ, Tonegawa S. Skeletal and CNS defects in Presenilin-1-deficient mice. Cell. 1997 May 16;89(4):629-39.
42. Wong PC, Zheng H, Chen H, Becher MW, Sirinathsinghji DJ, Trumbauer ME, et al. Presenilin 1 is required for Notch1 and DII1 expression in the paraxial mesoderm. Nature. 1997 May 15;387(6630):288-92.
43. Quon D, Wang Y, Catalano R, Scardina JM, Murakami K, Cordell B. Formation of beta-amyloid protein deposits in brains of transgenic mice. Nature. 1991 Jul 18;352(6332):239-41.
44. Moran PM, Higgins LS, Cordell B, Moser PC. Age-related learning deficits in transgenic mice expressing the 751-amino acid isoform of human beta-amyloid precursor protein. Proc Natl Acad Sci U S A. 1995 Jun 6;92(12):5341-5.
45. Higgins GA, Jacobsen H. Transgenic mouse models of Alzheimer's disease: phenotype and application. Behav Pharmacol. 2003 Sep;14(5-6):419-38.
46. Games D, Adams D, Alessandrini R, Barbour R, Berthelette P, Blackwell C, et al. Alzheimer-type neuropathology in transgenic mice overexpressing V717F beta-amyloid precursor protein. Nature. 1995 Feb 9;373(6514):523-7.
47. Masliah E, Sisk A, Mallory M, Mucke L, Schenk D, Games D. Comparison of neurodegenerative pathology in transgenic mice overexpressing V717F beta-amyloid precursor protein and Alzheimer's disease. J Neurosci. 1996 Sep 15;16(18):5795-811.
48. Chen G, Chen KS, Knox J, Inglis J, Bernard A, Martin SJ, et al. A learning deficit related to age and beta-amyloid plaques in a mouse model of Alzheimer's disease. Nature. 2000 Dec 21-28;408(6815):975-9.
49. Irizarry MC, Soriano F, McNamara M, Page KJ, Schenk D, Games D, et al. Abeta deposition is associated with neuropil changes, but not with overt neuronal loss in the human amyloid precursor protein V717F (PDAPP) transgenic mouse. J Neurosci. 1997 Sep 15;17(18):7053-9.
50. Hsiao K, Chapman P, Nilsen S, Eckman C, Harigaya Y, Younkin S, et al. Correlative memory deficits, Abeta elevation, and amyloid plaques in transgenic mice. Science. 1996 Oct 4;274(5284):99-102.
51. Irizarry MC, McNamara M, Fedorchak K, Hsiao K, Hyman BT. APPSw transgenic mice develop age-related A beta deposits and neuropil abnormalities, but no neuronal loss in CA1. J Neuropathol Exp Neurol. 1997 Sep;56(9):965-73.
52. Sturchler-Pierrat C, Abramowski D, Duke M, Wiederhold KH, Mistl C, Rothacher S, et al. Two amyloid precursor protein transgenic mouse models with Alzheimer disease-like pathology. Proc Natl Acad Sci U S A. 1997 Nov 25;94(24):13287-92.
53. Kelly PH, Bondolfi L, Hunziker D, Schlecht HP, Carver K, Maguire E, et al. Progressive age-related impairment of cognitive behavior in APP23 transgenic mice. Neurobiol Aging. 2003 Mar-Apr;24(2):365-78.
54. Calhoun ME, Wiederhold KH, Abramowski D, Phinney AL, Probst A, Sturchler-Pierrat C, et al. Neuron loss in APP transgenic mice. Nature. 1998 Oct 22;395(6704):755-6.
55. Duff K, Eckman C, Zehr C, Yu X, Prada CM, Perez-tur J, et al. Increased amyloid-beta42(43) in brains of mice expressing mutant presenilin 1. Nature. 1996 Oct 24;383(6602):710-3.
56. Herreman A, Hartmann D, Annaert W, Saftig P, Craessaerts K, Serneels L, et al. Presenilin 2 deficiency causes a mild pulmonary phenotype and no changes in amyloid precursor protein processing but enhances the embryonic lethal phenotype of presenilin 1 deficiency. Proc Natl Acad Sci U S A. 1999 Oct 12;96(21):11872-7.

57. Borchelt DR, Ratovitski T, van Lare J, Lee MK, Gonzales V, Jenkins NA, et al. Accelerated amyloid deposition in the brains of transgenic mice coexpressing mutant presenilin 1 and amyloid precursor proteins. Neuron. 1997 Oct;19(4):939-45.
58. Holcomb L, Gordon MN, McGowan E, Yu X, Benkovic S, Jantzen P, et al. Accelerated Alzheimer-type phenotype in transgenic mice carrying both mutant amyloid precursor protein and presenilin 1 transgenes. Nat Med. 1998 Jan;4(1):97-100.
59. Takeuchi A, Irizarry MC, Duff K, Saido TC, Hsiao Ashe K, Hasegawa M, et al. Age-related amyloid beta deposition in transgenic mice overexpressing both Alzheimer mutant presenilin 1 and amyloid beta precursor protein Swedish mutant is not associated with global neuronal loss. Am J Pathol. 2000 Jul;157(1):331-9.
60. Wirths O, Multhaup G, Czech C, Blanchard V, Moussaoui S, Tremp G, et al. Intraneuronal Abeta accumulation precedes plaque formation in beta-amyloid precursor protein and presenilin-1 double-transgenic mice. Neurosci Lett. 2001 Jun 22;306(1-2):116-20.
61. Schmitz C, Rutten BP, Pielen A, Schafer S, Wirths O, Tremp G, et al. Hippocampal neuron loss exceeds amyloid plaque load in a transgenic mouse model of Alzheimer's disease. Am J Pathol. 2004 Apr;164(4):1495-502.
62. Wirths O, Multhaup G, Czech C, Feldmann N, Blanchard V, Tremp G, et al. Intraneuronal APP/A beta trafficking and plaque formation in beta-amyloid precursor protein and presenilin-1 transgenic mice. Brain Pathol. 2002 Jul;12(3):275-86.
63. Blanchard V, Moussaoui S, Czech C, Touchet N, Bonici B, Planche M, et al. Time sequence of maturation of dystrophic neurites associated with A[beta] deposits in APP/PS1 transgenic mice. Experimental Neurology. 2003;184(1):247-63.
64. Franklin K, Paxinos G. The mouse brain in stereotaxic coordinates. San Diego: Academic Press. 1996.
65. Kantor O, Temel Y, Holzmann C, Raber K, Nguyen HP, Cao C, et al. Selective striatal neuron loss and alterations in behavior correlate with impaired striatal function in Huntington's disease transgenic rats. Neurobiol Dis. 2006 Feb 8.
66. Gundersen HJ, Jensen EB. The efficiency of systematic sampling in stereology and its prediction. J Microsc. 1987 Sep;147 (Pt 3):229-63.
67. Schmitz C, Hof PR. Design-based stereology in neuroscience. Neuroscience. 2005;130(4):813-31.
68. Schmitz C, Hof PR. Recommendations for straightforward and rigorous methods of counting neurons based on a computer simulation approach. J Chem Neuroanat. 2000 Oct;20(1):93-114.
69. Schmitz C. Variation of fractionator estimates and its prediction. Anat Embryol (Berl). 1998 Nov;198(5):371-97.
70. Wirths O, Multhaup G, Bayer TA. A modified beta-amyloid hypothesis: intraneuronal accumulation of the beta-amyloid peptide--the first step of a fatal cascade. J Neurochem. 2004 Nov;91(3):513-20.
71. Lee HG, Moreira PI, Zhu X, Smith MA, Perry G. Staying connected: synapses in Alzheimer disease. Am J Pathol. 2004 Nov;165(5):1461-4.
72. Gomez-Isla T, Price JL, McKeel DW, Jr., Morris JC, Growdon JH, Hyman BT. Profound loss of layer II entorhinal cortex neurons occurs in very mild Alzheimer's disease. J Neurosci. 1996 Jul 15;16(14):4491-500.
73. Giannakopoulos P, Herrmann FR, Bussiere T, Bouras C, Kovari E, Perl DP, et al. Tangle and neuron numbers, but not amyloid load, predict cognitive status in Alzheimer's disease. Neurology. 2003 May 13;60(9):1495-500.
74. Zhang Y, McLaughlin R, Goodyer C, LeBlanc A. Selective cytotoxicity of intracellular amyloid beta peptide1-42 through p53 and Bax in cultured primary human neurons. J Cell Biol. 2002 Feb 4;156(3):519-29.
75. El-Agnaf OM, Mahil DS, Patel BP, Austen BM. Oligomerization and toxicity of beta-amyloid-42 implicated in Alzheimer's disease. Biochem Biophys Res Commun. 2000 Jul 14;273(3):1003-7.
76. McLean CA, Cherny RA, Fraser FW, Fuller SJ, Smith MJ, Beyreuther K, et al. Soluble pool of Abeta amyloid as a determinant of severity of neurodegeneration in Alzheimer's disease. Ann Neurol. 1999 Dec;46(6):860-6.
77. Hartley DM, Walsh DM, Ye CP, Diehl T, Vasquez S, Vassilev PM, et al. Protofibrillar intermediates of amyloid beta-protein induce acute electrophysiological changes and progressive neurotoxicity in cortical neurons. J Neurosci. 1999 Oct 15;19(20):8876-84.
78. Billings LM, Oddo S, Green KN, McGaugh JL, LaFerla FM. Intraneuronal Abeta causes the onset of early Alzheimer's disease-related cognitive deficits in transgenic mice. Neuron. 2005 Mar 3;45(5):675-88.
79. Dickson DW. Building a more perfect beast: APP transgenic mice with neuronal loss. Am J Pathol. 2004 Apr;164(4):1143-6.

Auteursrechterlijke overeenkomst

Opdat de Universiteit Hasselt uw eindverhandeling wereldwijd kan reproduceren, vertalen en distribueren is uw akkoord voor deze overeenkomst noodzakelijk. Gelieve de tijd te nemen om deze overeenkomst door te nemen en uw akkoord te verlenen.

Ik/wij verlenen het wereldwijde auteursrecht voor de ingediende eindverhandeling:
Neuronal numbers in the frontal cortex of a novel transgenic mouse model of Alzheimer's Disease
Richting: **Master in de biomedische wetenschappen** Jaar: **2006**
in alle mogelijke mediaformaten, - bestaande en in de toekomst te ontwikkelen - , aan de Universiteit Hasselt.

Deze toekenning van het auteursrecht aan de Universiteit Hasselt houdt in dat ik/wij als auteur de eindverhandeling, - in zijn geheel of gedeeltelijk -, vrij kan reproduceren, (her)publiceren of distribueren zonder de toelating te moeten verkrijgen van de Universiteit Hasselt.

U bevestigt dat de eindverhandeling uw origineel werk is, en dat u het recht heeft om de rechten te verlenen die in deze overeenkomst worden beschreven. U verklaart tevens dat de eindverhandeling, naar uw weten, het auteursrecht van anderen niet overtreedt.

U verklaart tevens dat u voor het materiaal in de eindverhandeling dat beschermd wordt door het auteursrecht, de nodige toelatingen hebt verkregen zodat u deze ook aan de Universiteit Hasselt kan overdragen en dat dit duidelijk in de tekst en inhoud van de eindverhandeling werd genotificeerd.

Universiteit Hasselt zal u als auteur(s) van de eindverhandeling identificeren en zal geen wijzigingen aanbrengen aan de eindverhandeling, uitgezonderd deze toegelaten door deze licentie

Ik ga akkoord,

Marijke LEMMENS

Datum: